Numerical investigation of the effect of radiator placement on temperature distribution in a room

Hande Ufat

Vocational School of Technical Sciences, Air Conditioning and Refrigeration Department,
Bursa Uludag University
Bursa, Turkey
Email: handet@uludag.edu.tr

Abstract: This study analyses the impact of radiator placement on temperature distribution in a room using CFD analysis. Radiators are typically placed under windows or on outer walls. However, in the area under study, where there are large windows extending to the floor on the outer walls, the radiator was positioned on the empty inner wall. Two variations of the analysis were conducted using the ANSYS Fluent program. One variation involved a vertical installation of an aluminium panel radiator of the same length as the existing radiator on the outer wall next to one of the two windows. The other variation involved the installation of two radiators of the same length as the existing radiator next to the windows. The results showed that the room heated up faster when two radiators were used compared to other alternatives. Heating a room with two radiators of equal length and surface temperature results in a faster temperature increase. When a radiator is positioned vertically, the average temperature remains the same as the current situation. Using multiple smaller radiators instead of a single large one that provides the same amount of heat allowed the environment to warm up more quickly.

Keywords: CFD analysis; thermal comfort; panel radiator; temperature distribution.

Reference to this paper should be made as follows: Ufat, H. (2024) 'Numerical investigation of the effect of radiator placement on temperature distribution in a room', *Progress in Computational Fluid Dynamics*, Vol. 24, No. 6, pp.367–376.

Biographical notes: Hande Ufat is a Lecturer in Bursa Uludag University Vocational School of Technical Sciences, Air Conditioning and Refrigeration Department. She received her Master's and PhD in Mechanical Engineering Thermodynamics Science from Bursa Uludag University in 2011 and 2017, respectively. She is a researcher in the field of heating, ventilation and air conditioning (HVAC) systems and indoor air quality. She worked as a research assistant in Bursa Uludag University Mechanical Engineering Department between 2008–2017. She has been working as a Lecturer in Vocational School of Technical Sciences, Air Conditioning and Refrigeration Department in the same university since 2017.

This paper is a revised and expanded version of a paper entitled 'Investigation of the effect of panel radiator placement on temperature distribution in a room by CFD analysis' presented at 15th National Congress of Sanitary Engineering, Izmir, Turkey, 26–29 April 2023.

1 Introduction

Buildings account for 30–40% of global energy consumption. A large part of this energy consumption is used for heating (Ucler et al., 2015; Sarbu and Sebarchievici, 2015). Large energy savings can be achieved with small changes that can be made in these times of decreasing energy resources and increasing costs. Panel radiators are mostly used for heating buildings. Studies have shown that radiators as a central heating system give better results both in terms of thermal comfort and energy consumption compared to other systems (Sevilgen and Kilic, 2011). Parameters to be considered in terms of thermal comfort and energy consumption are: radiator surface area, operating temperature and placement in the room, barriers placed around the radiator, thermal conduction coefficients of the walls and window dimensions (Sevilgen and Kilic, 2011; Ucler et al., 2015). It is crucial to have a good understanding of these factors, from designers to users. Although different studies have been conducted depending on the type of radiator connection and the presence of obstacles around the radiator, the effect of radiator placement on heating has not been studied much. In their study, Ucler et al. (2015) experimentally investigated the effect of the obstacles placed around the radiator on the heating. They took measurements by covering the top and sides of a radiator placed under the window. Considering the temperature measurements taken in the middle of the room, the desired temperature was reached in a shorter time with a slight difference in the open radiators. Considering the energy consumed, there was no significant difference. Basok et al. (2014) solved the air distribution in a room

Copyright © 2024 Inderscience Enterprises Ltd.

heated by a two-panel radiator placed under a window using CFD analysis. They observed that the temperature distribution in the space is not uniform, and there are cold areas near the floor and the outer wall. Calisir et al. (2017) attempted to determine the best connection method by studying the flow characteristics in the radiators, both experimentally and with CFD analysis, when the water inlet and outlet temperature connections are in different locations in a panel radiator. They looked at three different connections: top-bottom-same end, top-bottom-opposite end and bottom-bottom-opposite end. For all water inlet temperatures tested, the top-bottom-opposite-end joint was found to radiate the most heat and provide the most uniform temperature distribution in the radiator. The results of the experimental study and the CFD analysis also overlap.

Sevilgen and Kilic (2011) conducted a study on the distribution of heat and humidity, as well as thermal comfort in a room heated by two panel radiators, using CFD analysis on a mannequin in different environmental conditions. The study was conducted with varying wall and window heat transmission coefficients. The results showed that in an environment with well-insulated walls and windows, thermal comfort increased while energy consumption decreased. Ganesh et al. (2020) conducted a numerical simulation to optimise the effect of panel and fan radiators on indoor air and people in an office room. The study also examined the effects of heat sources and objects in the environment on temperature distribution. The results showed that both types of radiators provided good temperature distribution from floor to ceiling, but the use of fan radiators is recommended for a better temperature gradient. It has been observed that objects do not prevent heat transfer, but they do affect air flow by creating turbulence in the surrounding areas.

The studies have analysed panel radiators with different pipe connection types, building construction materials, and obstacles placed around the radiator to determine their effectiveness on thermal comfort. However, the effect of temperature distribution in the room has not been analysed in terms of the different positioning of the same radiator. This study aims to examine the effect of a radiator of the same size and surface temperature on heating a room.

The temperature distribution in an existing space heated by a radiator was analysed using the Fluent program. The radiator is currently placed on the interior wall, but it is recommended to be on the exterior wall. The appropriately sized radiator should be installed vertically, taking into account the empty spaces on the external walls of the room. Alternatively, the possibility of placing two radiators, each half the size of the original radiator, in the gaps of the external wall was considered. The scenarios were then compared based on the same surface area and temperature. The aim of this research is to identify the optimal radiator location that will provide the most efficient temperature distribution in a given space. Achieving a faster heating time with the same radiator will enhance the thermal comfort of the occupants and reduce energy consumption. Future studies could incorporate human modelling and radiant heat transfer.

2 Material and method

2.1 The CFD room model

The 3D model of the existing room was created using ANSYS Workbench. The room measures 6 m × 4 m × 2.6 m and has two windows; window 1 measures 3 m × 2 m and window 2 measures 2 m × 2 m. The outer walls contain the windows, while the inner walls do not. The room is located on the mezzanine floor. The aluminium panel radiator measures 1.5 m × 0.6 m. Fresh air enters through a window and exits through an outlet located under the room door on the opposite wall. Please refer to Figure 1 for the current model.

Table 1 Specifications of geometry

Geometry (objects)	*Size (L × H × W)*	*Position*
Window 1	3 m × 2 m	Long side of the room
Window 2	2 m × 2 m	Short side of the room
Inner wall 1	2.1 m × 2.6 m	Near window 1
Inner wall 2	4 m × 2.6 m	Wall with outlet
Inner wall 3	6 m × 2.6 m	Opposite of window 1
Exterior wall 1	3.9 m × 2.6 m	Wall with window 1
Exterior wall 2	4 m × 2.6 m	Wall with window 2
Floor/ceiling	4 m × 6 m	
Inlet	1 m × 0.1 m	On the exterior wall 2
Outlet	1 m × 0.1 m	On the inner wall 2
Radiator (current situation)	1.5 m × 0.6 m × 0.1 m	On the inner wall 1
Radiator (scenario 1)	0.6 m × 1.5 m × 0.1 m	Left side of the window 2
Radiator 1 (scenario 2)	0.75 m × 0.6 m × 0.1 m	Left side of the window 2
Radiator 2 (scenario 2)	0.75 m × 0.6 m × 0.1 m	Left side of the window 1

The radiator is currently positioned horizontally on the inner wall next to window 1, 10 cm above the floor. In scenario one, the radiator is placed vertically to the left of window 2. In scenario two, two radiators of the same length as the existing one are added, one to the left of window 2 and the other to the left of window 1.

The models for the first and second scenarios are also presented in Figures 2 and 3. Additional details and dimensions can be found in Table 1.

Figure 1 Current situation model (see online version for colours)

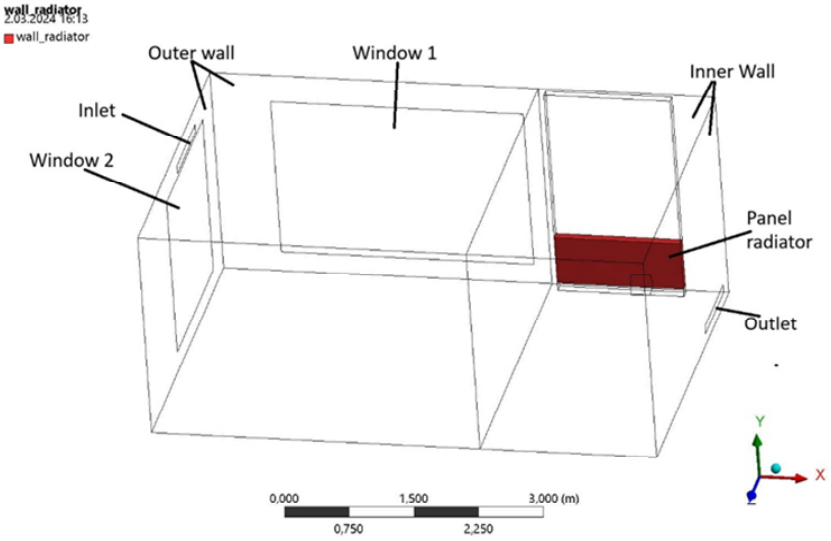


Figure 2 Model of the first scenario (see online version for colours)

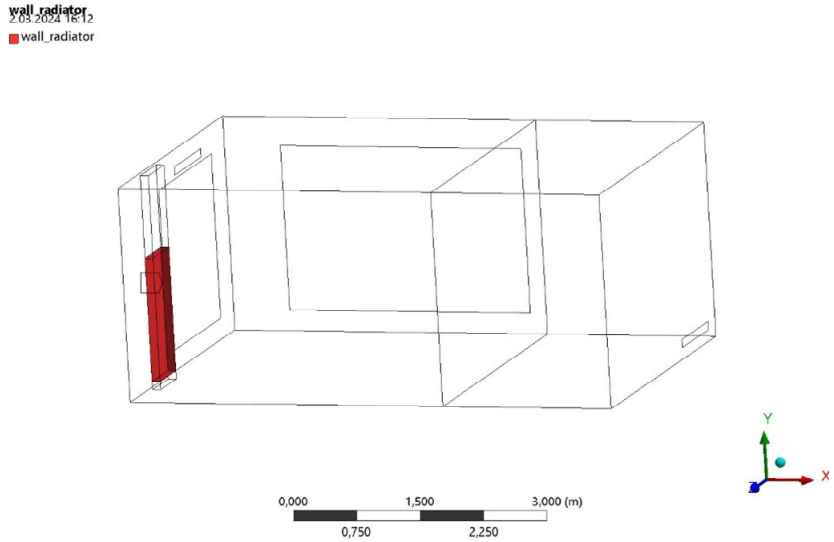


Figure 3 Model of the second scenario (see online version for colours)

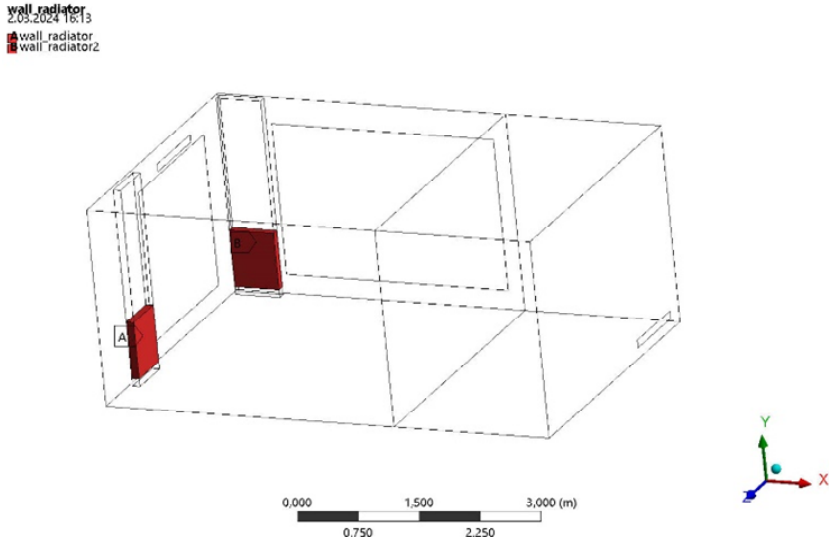
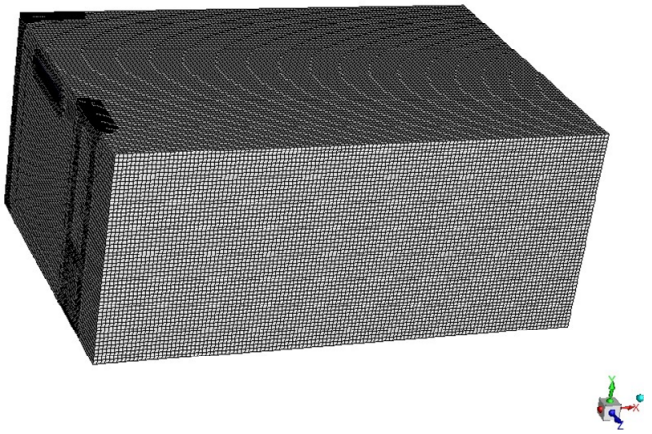
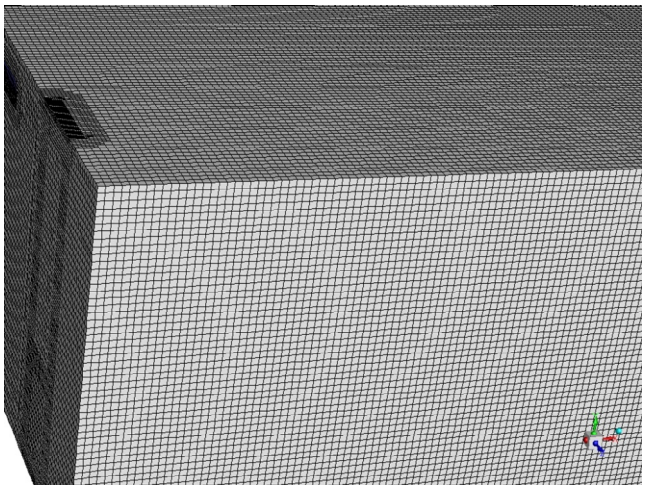


Figure 4 (a) Mesh model (b) Zoomed image of mesh model (see online version for colours)

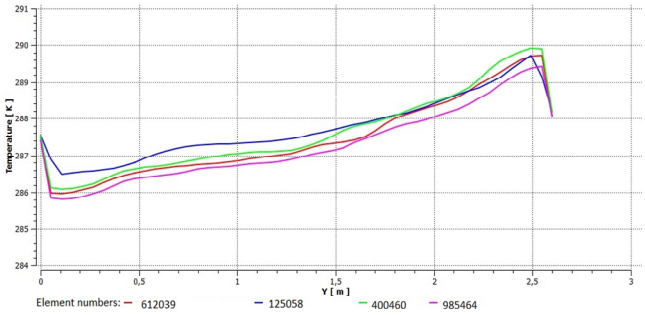


(a)



(b)

Figure 5 Temperature-room height graph at different mesh numbers (see online version for colours)



The quadratic mesh was chosen as it was deemed appropriate for the model. Figure 4(a) displays the mesh model. To ensure mesh independence, the analysis was performed at various mesh numbers and the graph of temperature change from ceiling to floor was plotted. A specific point was identified and is shown in Figure 5. A graph of temperature versus room height was obtained by running the analysis at mesh numbers of 125,058, 400,460, 612,039 and 985,464. Upon examining the graph, it is evident that the analyses conducted with mesh numbers of 612,039 and 985,564 are highly similar. Analyses were performed on 612,039 meshes to reduce the analysis time.

2.2 Governing equations and numerical methods

The Fluent program was utilised to conduct a three-dimensional analysis of flow and heat transfer. The program numerically solves the continuity, energy, and transport equations, taking into account natural convection effects. The numerical solution employs a second-order discretisation method and the SIMPLE algorithm.

The mass conservation equation can be written as the following:

$$\frac{\partial p}{\partial t}+\nabla\cdot\left(\rho\bar{v}\right)=S_m \tag{1}$$

Equation (1) is the general form of the mass conservation equation and is valid for both compressible and incompressible flows. The term S_m is the amount of mass that changes during the phase change.

Conservation of momentum is given in equation (2) as follows;

$$\frac{\partial p}{\partial t}\left(\rho\vec{v}\right)+\nabla\cdot\left(\rho\vec{v}\vec{v}\right)=-\nabla p+\nabla\cdot\left(\bar{\bar{\tau}}\right)+\rho\vec{g}+\vec{F} \tag{2}$$

The value of $\bar{\bar{\tau}}$ is the stress tensor and is calculated as follows.

$$\bar{\bar{\tau}}=\mu\left[\left(\nabla\vec{v}+\nabla\vec{v}^{T}\right)-\frac{2}{3}\nabla\cdot\vec{v}I\right] \tag{3}$$

μ is the molecular viscosity, p is the static pressure, and I is the unit tensor.

The energy conservation equation is given in the most general form as follows;

$$\begin{aligned}&\frac{\partial}{\partial t}(\rho E)+\nabla\cdot\left(\vec{v}\left(\rho\vec{v}+p\right)\right)\\&=\nabla\cdot\left(k_{eff}\nabla T-\left(\sum_j h_j\vec{J}_j+\left(\bar{\bar{\tau}}\cdot\vec{v}\right)\right)\right)+S_h\end{aligned} \tag{4}$$

k_{eff} is expressed as the effective transport coefficient. The term J_i is the diffusion coefficient of j species in multiphase flows. The first three terms on the right of equation (4) denote the energy transfer during transmission, species diffusion, and viscous distribution, respectively. The term S_h refers to the volumetric heat sources. The expression E can be found as follows;

$$E=h-\frac{p}{p}+\frac{v^2}{2} \tag{5}$$

The conservation equation for the species transport equation can be written in general form as follows;

$$\frac{\partial}{\partial t}\left(\rho Y_i\right)+\nabla\cdot\left(\rho\vec{v}Y_i\right)=\nabla\left[\left(\rho D_{i,m}+\frac{\mu_t}{Sc_t}\right)\nabla Y_i\right]+S_i \tag{6}$$

The Y_i value given in equation (6) is the local mass ratio in the i^{th} type, where D_{im} is the mass diffusion coefficient of type i in the mixture, Sc_t is the turbulent Schmidt number and S_i is any source term.

Although the standard k-ε model is preferred in many studies on indoor air thermal distribution (Ganesh et al., 2020; Verma and Sinha, 2014; Nada et al., 2016; Lin and Xu, 2013) it has some limitations (Murakami, 1991). Instead, RNG k-ε model is preferred because it yields more stable and precise results (Sevilgen and Kilic, 2011; Chen, 1995; Costa et al., 1999). Both models are derived from the Navier-Stokes equations and use similar equations, but include additional functions for k and ε.

$$\frac{\partial}{\partial t}(\rho k)+\frac{\partial}{\partial x_i}(\rho k u_i)=\frac{\partial}{\partial x_j}\left[\alpha_k \mu_{eff}\frac{\partial k}{\partial x_j}\right] +G_k+G_b-\rho\varepsilon-Y_M+S_k \tag{7}$$

$$\frac{\partial}{\partial t}(\rho \varepsilon)+\frac{\partial}{\partial x_i}(\rho \varepsilon u_i)=\frac{\partial}{\partial x_j}\left[\alpha_\varepsilon \mu_{eff}\frac{\partial \varepsilon}{\partial x_j}\right] +C_{1\varepsilon}\frac{\varepsilon}{k}(G_k+G_{3\varepsilon}G_b) -C_{2\varepsilon\rho}\frac{\varepsilon^2}{k}-R_\varepsilon+S_\varepsilon \tag{8}$$

G_k is the turbulent kinetic energy due to average velocity gradients. G_b is the turbulent kinetic energy due to the buoyancy force. Y_M is a wavy expansion distribution in compressible turbulence. α_k and α_ε are inverse Prandtl numbers for k and ε, respectively.

Turbulent viscosity in the RNG k-ε model;

$$d\left(\frac{\rho^2 k}{\sqrt{\varepsilon\mu}}\right)=1.72\frac{\hat{v}}{\sqrt{\hat{v}^3-1+C_v}}d\hat{v} \tag{9}$$

The ordinary differential equation seen in equation (9) improves the flow around the wall better with a low R_e number. In this equation, C_v is expressed as ≈100.

$$\hat{v}=\frac{\mu_{eff}}{\mu}$$

At high Reynolds number limits, from equation (9);

$$\mu_k=\rho C_\mu\frac{k^2}{\varepsilon} \tag{10}$$

The constants used in this model are C_μ, $C_{1\varepsilon}$, $C_{2\varepsilon}$ and their values are given $C_\mu = 0.0845$, $C_{1\varepsilon} = 1.42$, $C_{2\varepsilon} = 1.68$.

The heat transfer by radiation from surfaces was modelled using the surface-to-surface (S2S) model. The energy transfer between two surfaces is dependent on their area, distance, and position, which are determined by the vision factor, a geometric function. For more information on the surface-to-surface radiation model, refer to Raithby and Chui (1990).

The analysis was conducted for a duration of 30 minutes, with each file being solved using 3,600 time steps and a time step size of 0.5. This allowed for the examination of temperature distributions based on various radiator placements under identical boundary conditions and at the same time.

2.3 Boundary conditions

During the analysis, the surface temperature of the panel radiator was measured at 50°C. The inlet air velocity was 0.1 m/s, with a temperature of 5°C and a turbulence intensity of 10%. The outflow air was defined as the outlet. The outside temperature was also 5°C, and the initial temperature of the room was assumed to be the same as the outside temperature. The adjacent rooms to the interior walls, ceiling, and floor were considered unheated spaces, with a temperature of 15°C. The outer walls refer to the walls that are exposed to the external environment, which is assumed to be at a temperature of 5°C. Air-related properties were modelled using the Boussinesq model. The windows are double-glazed, with a density of 2,720 kg/m^3, specific heat (c_p) of 840 J/kgK, and a heat transmission coefficient of 0.7 W/mK. The inner walls have a density of 1,000 kg/m^3, a specific heat of 840 J/kgK, and a heat transmission coefficient of 0.46 W/mK. The outer walls have a density of 2,400 kg/m^3, a specific heat of 880 J/kgK, and a heat transmission coefficient of 2.5 W/mK. The radiators used are aluminium panel radiators. The heat convection coefficients were assumed to be 7 W/m^{2}K inside and 15 W/m^{2}K outside. The analysis includes the buoyancy effect because heated air rises spontaneously in natural convection. The radiator's surface temperature is given as 50°C. For the under floor heating analysis, the floor temperature is assumed to be 24°C.

3 Results and discussion

3.1 Validation of results

Ufat et al. (2017) previously published a study on the distribution of air temperature, velocity, and relative humidity in an operating room. The study measured these values at specific points, with temperature and relative humidity values taken from four points at a height of one meter from the ground. The devices used for measurement were connected via Wi-Fi and transmitted measurements taken per minute to the datalogger. The average of these measurements was then calculated. The measurements taken after the first hour were used to determine the room temperature during the steady-state regime. Upon comparing the measured data with the analysis results obtained from the Fluent program, it was observed that the data obtained were very similar.

3.2 Indoor temperature distribution obtained with the radiator placed on the inner wall

The 1.5 m long aluminium panel radiator is currently positioned on the inner wall of the room. Temperature distributions in the room were obtained after 30 minutes of heating using transient analysis under given boundary

conditions. Figure 6 shows the temperature distribution on the floor and outer wall, revealing a cold region in front of the windows and a cold outer wall surface of approximately 12–13°C. Figures 7 and 9 show a high temperature difference between the layers. For thermal comfort, the temperature difference from floor to ceiling should not exceed 3 degrees. However, in this case, the temperature difference is around 4–5 degrees.

Figure 6 Temperature distribution the floor and outer wall (see online version for colours)

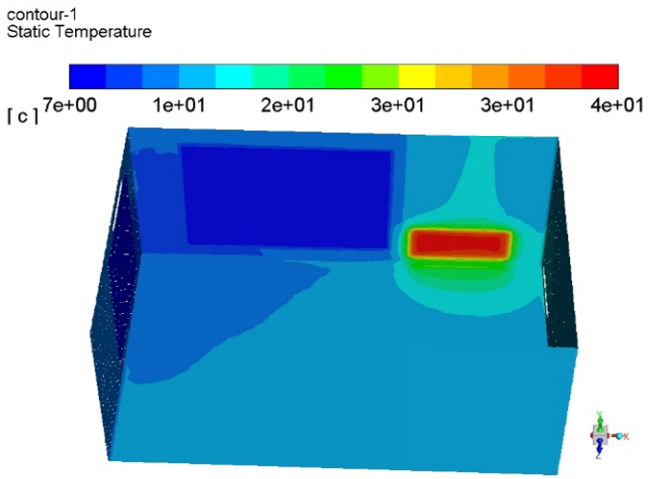
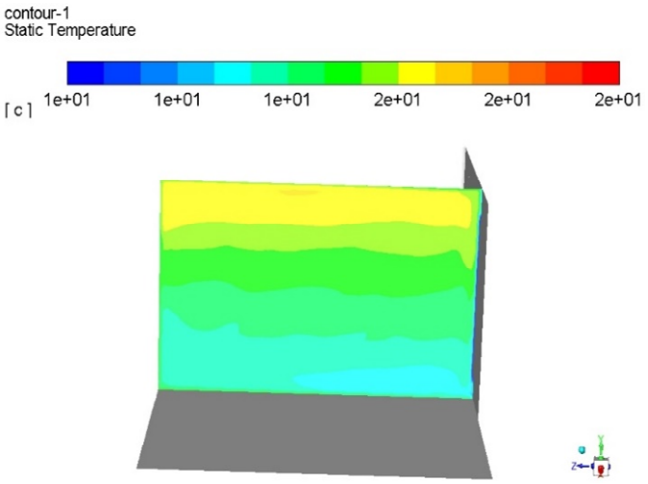


Figure 7 Temperature distribution on the middle of x coordinate (see online version for colours)



Figures 7 and 9 demonstrate that the room temperature is approximately 13°C up to the middle. A transient analysis was performed for 30 minutes, starting with an outdoor temperature of 5°C. As heated air rises, the temperature towards the ceiling reaches 19°C. Upon examining the temperature distribution on the floor, it is evident that the window fronts remain significantly cooler than the rest of the room.

3.3 Indoor temperature distribution obtained with the radiator placed vertically next to the window

Due to the lack of outer wall distance, the radiator of the same length in its current position is placed vertically next to the window, as shown in Figure 2. After the first 30 minutes of heating, a transient analysis was performed to determine the temperature distribution in the room.

Figure 8 Temperature distribution on the middle of y coordinate (see online version for colours)

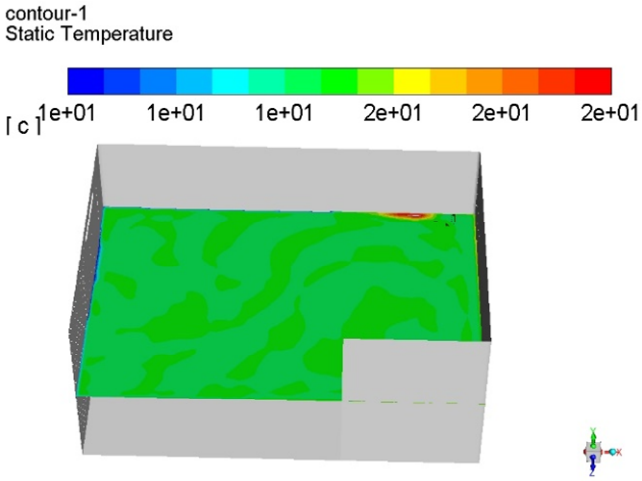


Figure 9 Temperature distribution on the middle of z coordinate (see online version for colours)

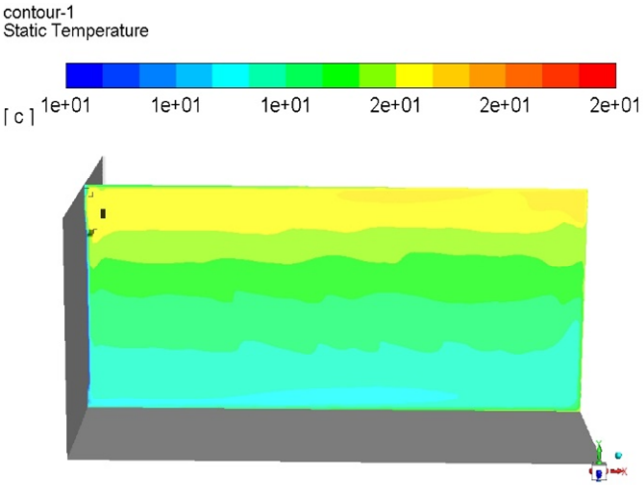


Figure 10 Temperature distribution the floor and walls (see online version for colours)

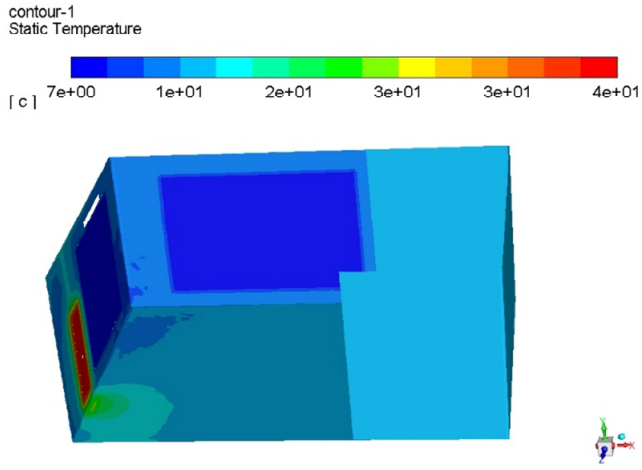


Figure 11 Temperature distribution on the middle of x coordinate (see online version for colours)

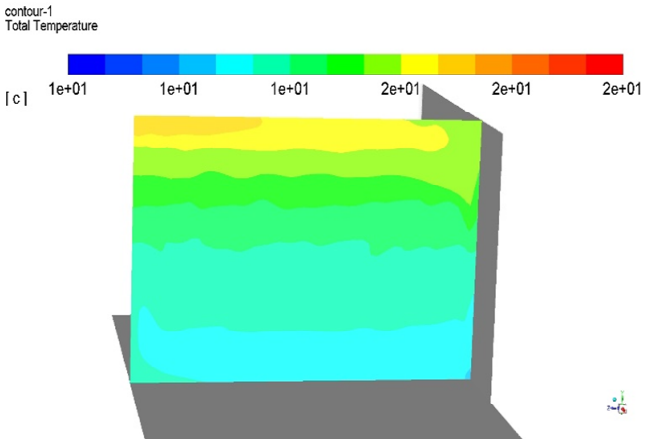


Figure 12 Temperature distribution on the middle of y coordinate (see online version for colours)

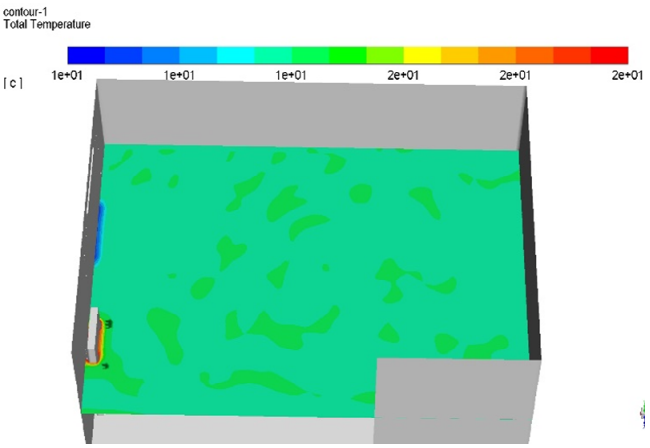
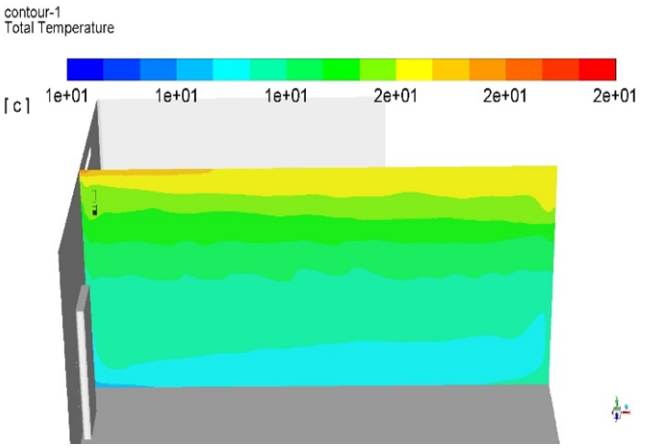


Figure 13 Temperature distribution on the middle of z coordinate (see online version for colours)



The temperature distributions in the middle section of the room are similar to the current situation, except for a slightly higher air temperature towards the ceiling (Figures 11–13). The higher temperature towards the ceiling is likely due to vertical positioning. Additionally, the floor temperature in front of the window is higher than the current situation (Figure 10). It is important to note that floor temperatures in living rooms can significantly affect foot temperature, which is important for human comfort. Therefore, the quicker the floor heats up, the more comfortable the indoor environment will be. Upon examining the temperature distribution on the outer walls in Figure 10, it is evident that the wall with the radiator is warmer, as expected, with an average temperature of 16°C. Conversely, the other outer wall remains cold, similar to the current situation, with a temperature of approximately 13°C.

Figure 14 Temperature distribution the floor and walls (see online version for colours)

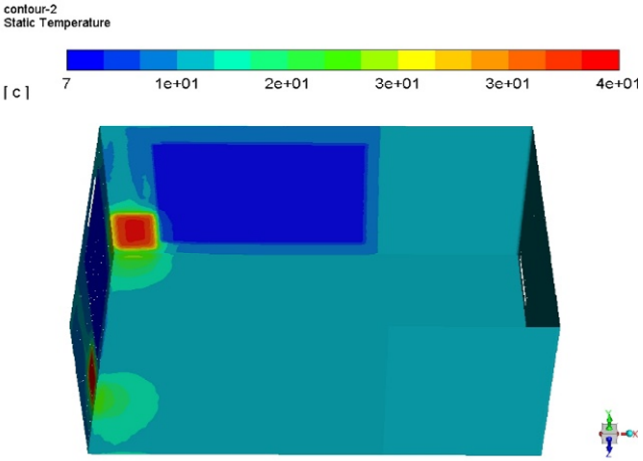
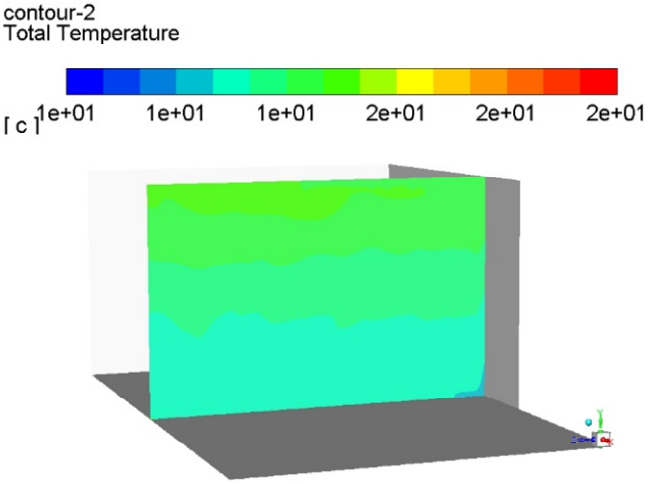


Figure 15 Temperature distribution on the middle of x coordinate (see online version for colours)



3.4 Indoor temperature distribution obtained by positioning two radiators near a window

Figure 3 shows that two radiators, of the same length as the current radiator, were positioned on both sides of the outer window. Transient analysis was then carried out, and temperature distributions on different planes and surfaces are presented.

Figures 15 and 17 show that the room temperature is more homogeneous in the middle of the room and higher compared to the other two analyses. Additionally, the vertical temperature difference is around 2 degrees, which is desirable for thermal comfort. Upon examining the temperature distribution on the floor in Figure 14, it is

evident that it is at a higher temperature than the other scenarios. This is due to the higher surface temperature of one of the outer walls, which in turn reduces the heat loss that would occur in that area.

Figure 16 Temperature distribution on the middle of y coordinate (see online version for colours)

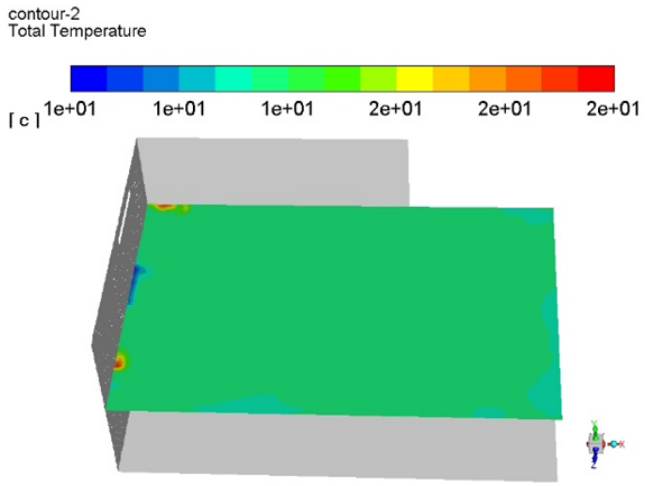


Figure 17 Temperature distribution on the middle of z coordinate (see online version for colours)

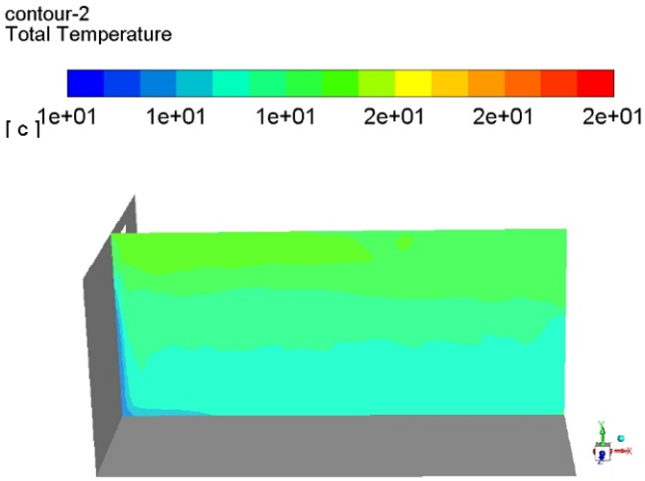
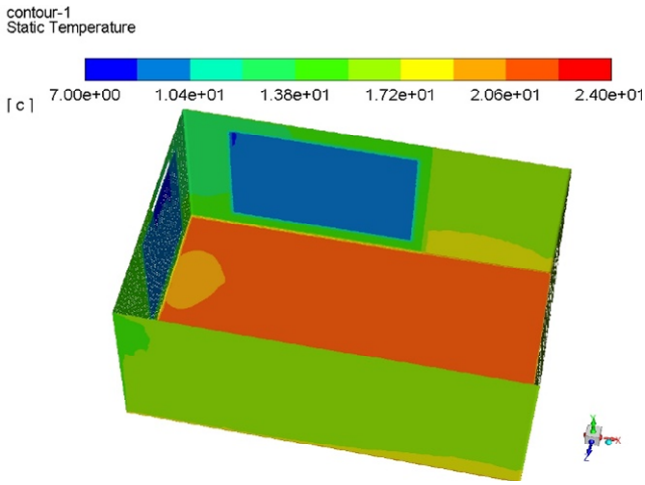


Figure 18 Temperature distribution on the floor and the walls (see online version for colours)



3.5 Floor heating

For existing spaces with under floor heating, Figure 18 displays the temperature distribution on the floor and walls. Figures 19, 20, and 21 display the temperature distribution at the midpoint of the x, y, and z coordinates of the plane, respectively.

Figure 19 Temperature distribution on the middle of the x coordinate (see online version for colours)

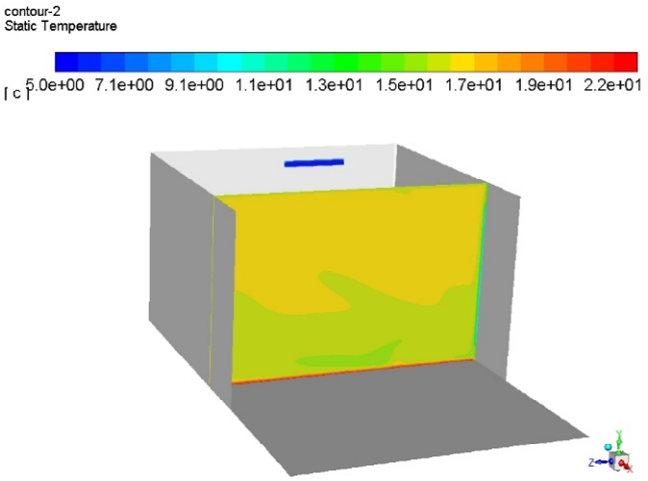
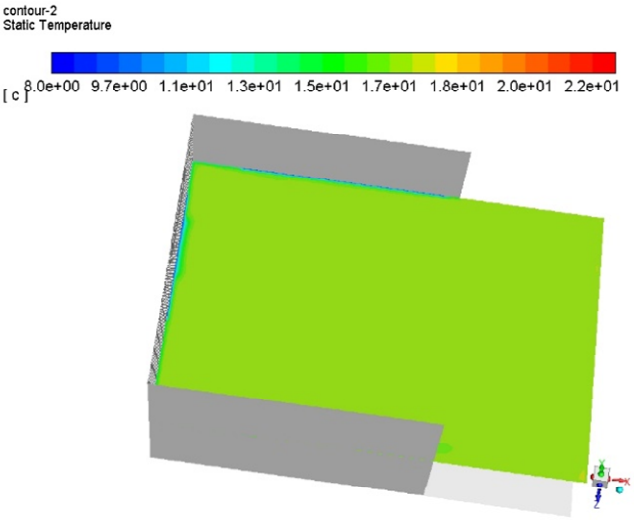


Figure 20 Temperature distribution on the middle of y coordinate (see online version for colours)

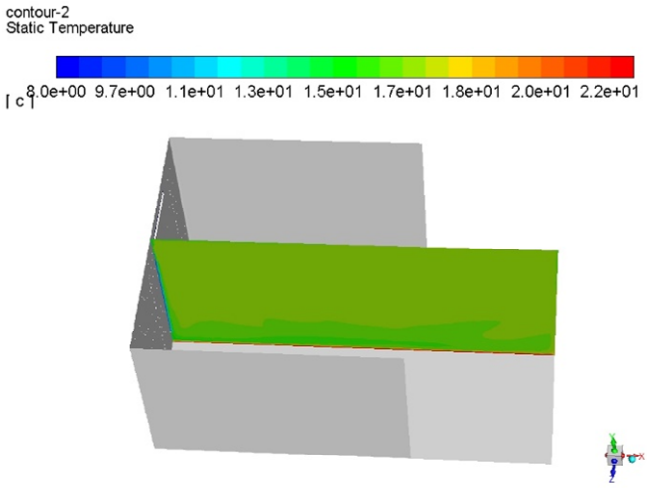


The analysis was conducted transiently and for the same duration as in the other analysis. Upon evaluation of the results, it is evident that the location is heated on average by 2°C more during the same period compared to heating with a radiator. While heating with radiators results in a more layered temperature distribution, under floor heating results in a more homogeneous temperature distribution. Additionally, the outer walls' temperature is higher than in all scenarios with a radiator (see Figure 18).

The temperature distribution resulting from heating the room for the first 30 minutes with the radiator at a surface temperature of 50 degrees is determined. The evaluation excludes subjective assessments unless clearly marked as such. Two scenarios are considered: in the first scenario, the

radiator is positioned vertically with the same length and surface temperature; in the second scenario, the radiator is positioned next to the exterior window.

Figure 21 Temperature distribution on the middle of z coordinate (see online version for colours)



The analysis produced values that closely resemble the current temperature distribution. However, it revealed that the floor was heated more.

In scenario 2, two 0.75 m long radiators were placed next to the exterior walls, with a total length identical to the others (1.5 m). The surface temperature of these radiators was also 50 degrees. The analysis showed that the room temperature increased by approximately 2 degrees more in 30 minutes.

The temperature difference between the floor and ceiling is lower in the baseline and scenario 1. Under floor heating yielded better results than radiator heating. Additionally, the room reached higher temperatures in the same period of time.

4 Conclusions

This study conducted CFD analyses in various scenarios at an existing location to shed light on how panel radiators can be positioned in areas with large windows. Transient analysis was performed with the same warm-up time for each scenario. The analyses determined temperature distributions in the space, and the results were examined by taking sections from specific locations in the space. The temperature distributions of the radiator on the inner wall next to one of the large windows and the vertically positioned radiator at the same level are similar due to the lack of sufficient distance on the outer wall. However, the ground temperature is higher during the same period. It is worth noting that the temperature of the ground in contact with the feet is high in the living environment. Placing two radiators of the same length on either side of the window increases the room temperature by almost 2°C and achieves a more homogeneous temperature distribution. It is recommended to place smaller panel radiators at several points instead of a single large panel radiator in spaces with large windows to allow the space to warm up more quickly. Energy conservation is crucial in today's world. Implementing small measures can have a significant impact on a large scale. Under floor heating has been analysed and proven to increase the environment's temperature by an average of 2–3°C compared to other scenarios. To ensure optimal thermal comfort, it is recommended to maintain a temperature difference of no more than 3 degrees between the floor and ceiling. Under floor heating achieves a better temperature distribution compared to heating with radiators. It is particularly suitable for spaces with large windows as it increases the ambient temperature more quickly. However, radiators can provide the same heating at a similar time with much less hot water, resulting in lower energy consumption. It is necessary to pay attention to the selection of the system and the good evaluation of the system in itself by evaluating the purpose of use, investment and operating costs and comfort conditions of the spaces.

Acknowledgements

Analysis was performed and the manuscript of the paper was written by Hande Ufat.

References

Basok, B.I., Davydenko, B.V., Farenuyk, G.G. and Goncharuk, S.M. (2014) 'Computational modeling of the temperature regime in a room with a two-panel radiator', *Journal of Engineering Physics and Thermophysics*, Vol. 87, No. 1, pp.1433–1438.

Calisir, T., Yazar, H.O. and Baskaya, S. (2017) 'Determination of the effects of different inlet-outlet locations and temperatures on PCCP panel radiator heat transfer and fluid flow characteristics', *International Journal of Thermal Sciences*, Vol. 121, pp.322–335, https://doi.org/10.1016/j.ijthermalsci.2017.07.026.

Chen, Q. (1995) 'Comparison of different k-ε models for indoor air flow computations', *Numerical Heat Transfer, Part B Fundamentals*, Vol. 28, No. 3, pp.353–369, https://doi.org/10.1080/10407799508928838.

Costa, J.J., Oliveira, L.A. and Blay, D. (1999) 'Test of several versions for the k-ε type turbulence modelling of internal mixed convection flows', *International Journal of Heat and Mass Transfer*, Vol. 42, No. 23, pp.391–4409, https://doi.org/10.1016/S0017-9310(99)00075-7.

Ganesh, G.A., Sinha, S.L. and Verma, T.N. (2020) 'Numerical simulation for optimization of the indoor environment of an occupied office building using double-panel and ventilation radiator', *Journal of Building Engineering*, Vol. 29, p.101139, https://doi.org/10.1016/j.jobe.2019.101139.

Lin, Y.J. and Xu, Z.Y. (2013) 'Buoyancy-driven flows by a heat source at different levels', *International Journal of Heat and Mass Transfer*, Vol. 58, Nos. 1–2, pp.312–321, https://doi.org/10.1016/j.ijheatmasstransfer.2012.11.008.

Murakami, S. (1991) 'Numerical prediction of horizontal nonisothermal 3-D jet in room based on the k-ε model', *ASHRAE Transactions*, Vol. 97, No. 1, pp.38–48, https://doi.org/10.18948/shase.26.82_101.

Nada, S.A., El-Batsh, H.M., Elattar, H.F. and Ali, N.M. (2016) 'CFD investigation of airflow pattern, temperature distribution and thermal comfort of UFAD system for theater buildings applications', *Journal of Building Engineering*, Vol. 6, pp.274–300, https://doi.org/10.1016/j.jobe.2016.04.008.

Raithby, G.D. and Chui, E.H. (1990) 'A finite-volume method for predicting a radiant heat transfer in enclosures with participating media', *ASME Journal of Heat and Mass Transfer*, Vol. 112, No. 2, pp.415–423, https://doi.org/10.1115/1.2910394.

Sarbu, I. and Sebarchievici, C. (2015) 'A study of the performances of low-temperature heating systems', *Energy Efficiency*, Vol. 8, pp.609–627 [online] https://link.springer.com/article/10.1007/s12053-014-9312-4.

Sevilgen, G. and Kilic, M. (2011) 'Numerical analysis of air flow, heat transfer, moisture transport and thermal comfort in a room heated by two-panel radiators', *Energy and Buildings*, Vol. 43, No. 1, pp.137–146, https://doi.org/10.1016/j.enbuild.2010.08.034.

Ucler, K., Kibar, A., Karabag, B. and Yigit, K.S. (2015) 'Mekân içerisinde pencere altinda bulunan radyatörlerin etrafina yerleştirilen engellerin deneysel olarak incelenmesi', *Makine Teknolojileri Elektronik Dergisi*, Vol. 12, No. 4, pp.61–69 [online] https://www.acarindex.com/pdfler/acarindex-1ae886a0-3dbc.pdf.

Ufat, H., Kaynakli, O., Yamankaradeniz, N. and Yamankaradeniz, R. (2017) 'Three-dimensional air distribution analysis of different outflow typed operating rooms at different inlet velocities and room temperatures', *Advances in Mechanical Engineering*, Vol. 9, No. 7, pp.1–12, https://doi.org/10.1177/168781401770741.

Verma, T.N. and Sinha, S.L. (2014) 'Contaminant control in intensive care unit of hospital', in *Applied Mechanics and Materials*, Vol. 592, pp.2489–2490, https://doi.org/10.4028/www.scientific.net/AMM.592-594.2486.